ORGANOMETALLICS

Article

pubs.acs.org/Organometallics

Probing the Structure of Methylalumoxane (MAO) by a Combined Chemical, Spectroscopic, Neutron Scattering, and Computational Approach

Fabio Ghiotto,[†] Chrysoula Pateraki,[†] Jukka Tanskanen,[‡] John R. Severn,[§] Nicole Luehmann,[∥] André Kusmin,[∥] Jörg Stellbrink,*[,∥] Mikko Linnolahti,*[,‡] and Manfred Bochmann*[,†]

[†]Wolfson Materials and Catalysis Centre, School of Chemistry, University of East Anglia, Norwich, United Kingdom

[‡]Department of Chemistry, University of Eastern Finland, Joensuu Campus, FI-80101 Joensuu, Finland

[§]UHM_wPE Chemistry & Catalysis, DSM, NL-6160MD Geleen, The Netherlands

[∥]Jülich Centre for Neutron Science and Institute for Complex Systems, Forschungszentrum Jülich, D-52425 Jülich, Germany

Supporting Information

ABSTRACT: The composition of methylalumoxane (MAO) and its interaction with trimethylaluminum (TMA) have been investigated by a combination of chemical, spectroscopic, neutron scattering, and computational methods. The interactions of MAO with donor molecules such as THF, pyridine, and PPh_3 as a means of quantifying the content of "free" and "bound" TMA have been evaluated, as well as the ability of MAO to produce $[Me_2AlL_2]^+$ cations, a measure of the electrophilic component likely to be involved in the activation of single-site catalysts. THF, pyridine, and diphenylphosphinopropane (dppp) give the corresponding TMA−donor ligand complexes accompanied by the formation of $[Me_2AlL_2]^+$ cations. The results suggest that MAO contains not only Lewis acid sites but also structures capable of acting as sources of $[AlMe_2]^+$ cations. Another unique, but still unresolved, structural aspect of MAO is the nature of "bound" and "free" TMA. The addition of the donors $OPPh_3$, PMe_3, and PCy_3 leads to the precipitation of polymeric MAO and shows that about one-fourth of the total TMA content is bound to the MAO polymers. This conclusion was independently confirmed by pulsed field gradient spin echo (PFG-SE) NMR measurements, which show fast and slow diffusion processes resulting from free and MAO-bound TMA, respectively. The hydrodynamic radius R_h of polymeric MAO in toluene solutions was found to be 12 ± 0.3 Å, leading to an estimate for the average size of MAO polymers of about 50−60 Al atoms. Small-angle neutron scattering (SANS) resulted in the radius R_S = 12.0 ± 0.3 Å for the MAO polymer, in excellent agreement with PFG-SE NMR experiments, a molecular weight of 1800 ± 100, and about 30 Al atoms per MAO polymer. The MAO structures capable of releasing $[AlMe_2]^+$ on reaction with a base were studied by quantum chemical calculations on the MAO models $(OAlMe)_n(TMA)_m$ for up to n = 8 and m = 5. Both −O−$AlMe_2$−O− and −O−$AlMe_2$−μ-Me− four-membered rings are about equally likely to lead to dissociation of $[AlMe_2]^+$ cations. The resulting MAO anions rearrange, with structures containing separated Al_2O_2 4-rings being particularly favorable. The results support the notion that catalyst activation by MAO can occur by both Lewis acidic cluster sites and $[AlMe_2]^+$ cation formation.

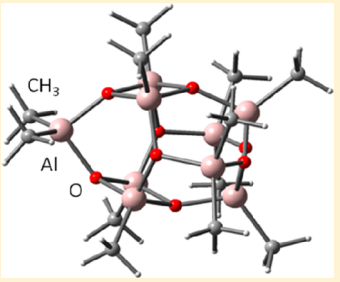

INTRODUCTION

Methylalumoxane (MAO), the product of the controlled hydrolysis of trimethylaluminum (TMA), is a widely used catalyst activator for olefin oligomerizations and polymerizations.[1,2] However, despite its important industrial use, little is known about the structure, due to a complex set of equilibria and to the lack of isolable components that are amenable to structural characterization.[3−6] In solution-phase catalysts MAO is typically employed at Al/transition-metal ratios on the order of $(10^3−10^4)/1$,[7] although Al/metal ratios of over 300000/1 have been reported.[8] MAO therefore contributes significantly to the operating costs of polymerization processes.[9] Over the last 30 years there have been many experimental and computational attempts to shed light on the constitution of MAO, to find a cheaper alternative or to improve its solubility and stability, but a fuller understanding of the chemistry involved has still not been achieved.[4−7,10−17]

In the simplest analysis, solutions of MAO consist of two different components: a polymeric MAO fraction, with a chemical formula often written as $[−Al(CH_3)O−]_n$ or as $[Al(CH_3)_{1.4−1.5}O_{0.75−0.80}]_n$, and residual TMA.[2,11,15−18] The molecular weights assumed or proposed for MAO range typically from about 700 (ca. 12 Al atoms)[1a,15a] to aggregates of 150−200 Al atoms (MW 9000−18000).[6h] Although many structures have been proposed without reaching a consensus, cages with 4-coordinated Al and 3-coordinated O centers are the most favored,[19] including nanotube-like structures.[2,16] This was

Received: April 5, 2013

   dx.doi.org/10.1021/om4002878 | Organometallics XXXX, XXX, XXX−XXX

supported by DFT calculations[13,15] and multinuclear NMR studies.[3,4] Barron synthesized a number of *tert*-butyl aluminoxane clusters as MAO models, such as $[^t\mathrm{BuAl}(\mu_3\text{-O})]_6$, which were amenable to structural characterization.[20] They were able to activate metallocenes to give catalysts of modest activity. The catalytic activity was found to be improved by adding TMA.[21]

TMA Determination. The TMA content has a strong influence on the catalytic properties of MAO. High amounts of TMA cause a decrease in catalyst activity[7,22,23] and the molecular weight of the polymer, in addition to having a strong influence on copolymerizations.[15a,24] TMA may be trapped by adding 2,6-di-*tert*-butyl-4-methylphenol (BHT) to MAO solutions to minimize chain transfer to aluminum and the leaching of the supported catalysts promoted by TMA.[25−27] For this reason, an accurate determination of the residual TMA content is crucial, especially considering that it is the only species clearly recognizable spectroscopically in MAO solutions. Various methods have been reported in the literature, but a systematic comparison and a study on their reliability and reproducibility are lacking. The TMA content can be determined by visual titration with pyridine in the presence of phenazine as an indicator.[28] This method, which is still widely used, can give exaggerated TMA values due to the reaction of pyridine not only with TMA but also with MAO polymers.[18] NMR techniques have proven to be more reliable and faster to use. The direct quantification of TMA in the ^{1}H NMR spectrum of MAO solutions is difficult due to overlapping TMA and MAO signals, even if estimates can be obtained.[29] The TMA content can be better measured by adding THF to give the adduct $Me_3Al{\cdot}THF$, the methyl protons of which are shifted to higher field in comparison to those of TMA, making signal integration easier.[18] However, the influence of the quantity of THF added on the TMA value obtained has not been explored. Another method for TMA determination consists of adding PPh_3 in known excess.[30] The ^{31}P NMR chemical shift is the weighted average of free and Me_3Al-bound PPh_3, and the TMA content is determined using a calibration curve. However, there are at least two different calibration curves in the literature,[4b,30] and a comparison of this method with that based on THF was not established.

Nature of TMA in MAO. The nature of the TMA−MAO interaction remains controversial. TMA is present in MAO solutions as the dimer $Al_2(\mu\text{-Me})_2Me_4$. However, there are different views of its interaction with MAO. Tritto et al. reported a low-temperature NMR study on MAO samples showing that TMA is mainly bound to MAO, and an analysis of the line broadening of the "sharp" Al−methyl signal suggested that it consisted of contributions from both free TMA and TMA binding to and exchanging with MAO.[4b] In contrast, FT-IR spectroscopic studies by Ystenes et al. suggested that there was no reaction between TMA (or Al_2Me_6) and MAO.[15a,31]

Literature reports distinguish between two forms of TMA in MAO: a fraction that can be removed under vacuum ("free" TMA), and a form of TMA that can only be removed chemically ("associated" or "bound" TMA).[1,2] For the "bound" TMA the following equilibrium is invoked:[13,15b]

$$(\mathrm{AlOMe})_n + (m/2)(\mathrm{AlMe_3})_2 \rightleftharpoons (\mathrm{AlOMe})_n(\mathrm{AlMe_3})_m$$

Moreover, the possibility was suggested that TMA molecules might be occluded inside the MAO cages, in order to explain why it is not possible to remove TMA quantitatively under vacuum. The addition of diethyl ether to MAO solutions in toluene was reported to lead to phase separation, with the upper phase containing all the TMA and some MAO and the lower phase containing most of the MAO. This process is reversible: i.e., the lower phase redissolves slowly on addition of TMA and toluene.[1a,32]

Activation Process. The ability of MAO to activate catalysts depends on the presence of Lewis acidic sites. EPR spectroscopic studies with TEMPO (2,2,6,6-tetramethylpiperidine-*N*-oxyl) as a spin probe have suggested at least two types of such sites, attributed to $-OAlMe_2$ and $-O_2AlMe$ structure fragments.[12a] Since cages based on 4-coordinate Al contain no coordinatively unsaturated centers, cleavage of an Al−O bond of a strained Al_2O_2 4-membered ring during the catalyst activation step has been suggested ("latent Lewis acidity").[20] More recently, a patent proposed another catalyst activation mode by invoking the formation of $[AlMe_2]^+$ cations during the interaction of metallocene catalyst precursors with MAO,[33,34] a suggestion that follows from the earlier preparation by Klosin et al. of $[AlMe_2(OEt_2)_2]^+$ salts and their use as catalyst activators.[35] It should be noted, however, that nonsolvated $[AlMe_2]^+$ is extremely unstable and reactive.[36]

Further information about the structure of MAO and of the mode of action of this industrially important activator is therefore urgently needed. We report here a multidisciplinary approach to determining the role of TMA in MAO formulations ("free" versus "bound") and the species involved in catalyst activation by chemical, NMR spectroscopic, and neutron-scattering methods, coupled with a computational interrogation of MAO models and their propensity for ionization into $[MAO]^-$ and $[AlMe_2]^+$.

RESULTS AND DISCUSSION

Interaction of MAO with O and N Donors. The first step in the characterization of MAO is the determination of the TMA content. The addition of increasing quantities of tetrahydrofuran (THF, $pK_b = 5$)[37] to MAO (30% solution in toluene) was studied by ^{1}H NMR spectroscopy (Figure 1).

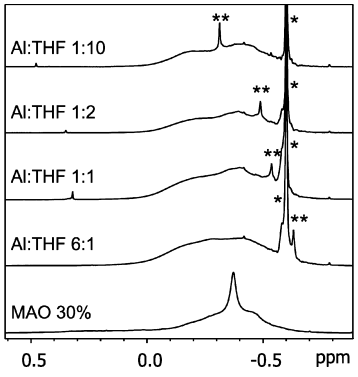

Figure 1. ^{1}H NMR spectra of MAO with increasing quantities of THF. The Al/THF ratio is reported as total Al present in the sample. A single asterisk (*) denotes the $AlMe_3{\cdot}$THF signal, and two asterisks (**) denote the $[Me_2Al(THF)_2]^+$ peak.

THF cleaves Al_2Me_6 to give $AlMe_3{\cdot}$THF, with a signal shift to higher field (ca. δ −0.6), which facilitates integration and quantification of the TMA content (Table 1). On THF addition the MAO signal is shifted to higher field. For Al/THF ratios between 1/1 and 1/10, the calculated TMA content of the samples of MAO is consistent and reproducible at ca. 3.3 ± 0.1 wt %. This is in agreement with data by Imhoff et al., who reported that the optimal ratio Al/THF to determine the TMA content is 1/4.[18,38]

dx.doi.org/10.1021/om4002878 | *Organometallics* XXXX, XXX, XXX−XXX

Table 1. TMA and $[Me_2Al(L)_2]^+$ Content of the MAO Sample as a Function of L and the TMA/L Ratio (L = THF, py)

	L = THF			L = py		
Al/L ratio	TMA (wt %)	TMA (mol/L)	$[Me_2AlL_2]^+$ (mol/L)	TMA (wt %)	TMA (mol/L)	$[Me_2AlL_2]^+$ (mol/L)
6/1	2.8	0.35	0.08	2.2	0.28	0.11
1/1	3.3	0.41	0.12	3.3	0.41	0.11
1/2	3.4	0.42	0.12	3.6	0.45	0.12
1/5	3.2	0.40	0.12	3.4	0.42	0.14
1/10	3.4	0.42	0.12	3.6	0.45	0.16
1/15	3.1	0.39	0.09	2.3	0.29	0.09
1/26	2.7	0.34	0.06	2.1	0.26	0.06

A newly emerging peak (labeled ** in Figure 1) appears on THF addition. When $[AlMe_2(THF)_2][MeB(C_6F_5)_3]$ is added to the solutions with Al/THF = 1/2 or 1/10, the intensity of this peak increases while its chemical shift does not change; it is therefore assigned to the cationic complex $[Me_2Al(THF)_2]^+$.[33] The assignments were further confirmed by calculated ^{1}H NMR chemical shifts (see the Supporting Information). This signal originates from a species to high field of TMA, at δ −0.7, and moves to δ −0.3 at higher THF concentrations;[39] the nature of this species was explored by modeling (vide infra).

Similar results were obtained on adding pyridine (py). Again formation of a cation, $[Me_2Al(py)_2]^+$, was observed. Table 1 shows the results of TMA and $[Me_2AlL_2]^+$ quantification for THF and pyridine. Within experimental error both methods give comparable results (3.3 ± 0.1 wt % TMA).

For Al/py = 6/1, the low TMA value can be tentatively explained by insufficient pyridine to extract the TMA quantitatively and to shift. For a large excess of pyridine, the ^{1}H NMR spectra show new signals at ca. δ 0.15, −0.30, and −0.55, indicating the formation of side products, which may account for the lower TMA values calculated for high [py]. The concentration of $[Me_2Al(py)_2]^+$ increases with the [py] for Al/py ratios between 1/1 and 1/10. These results explain why the literature method for TMA determination by pyridine/phenazine titration gives values higher than expected,[28] as pyridine does not simply form a 1/1 complex with TMA. The higher relative concentrations of $[Me_2Al(py)_2]^+$ found at high Al/py ratios indicate the preferential binding of pyridine to the more Lewis acidic cation-generating center.

Interaction of MAO with Phosphines. Other bases, such as phosphines, show variable degrees of interaction with MAO. There is no formation of $[Me_2Al(L)_2]^+$ cations when L = PPh_3 is added. We have established a new correlation for [TMA] determinations with PPh_3 in non-deuterated toluene (eq 1),

$$Al/P = -0.2957\delta - 1.5378 \quad R = 0.997 \qquad (1)$$

where *Al* indicates the moles of $AlMe_3(PPh_3)$ and *P* the moles of PPh_3 added to the solution (see the Supporting Information). The data are in good agreement with those obtained by the pyridine and THF methods, showing that the $[Me_2AlL_2]^+$ cations do not arise from TMA.

The diphosphines 1,1-diphenylphosphinomethane (dppm), 1,2-diphenylphosphinoethane (dppe), and 1,3-diphenylphosphinopropane (dppp) show variable tendencies to form $[Me_2AlL_2]^+$ adducts (Figure 2). Adding dppm leaves the shape of the MAO ^{1}H NMR signal unaffected, and there is little detectable interaction. Increasing quantities of dppe sharpen the TMA signal at δ −0.3, but there is no formation of a cationic species.

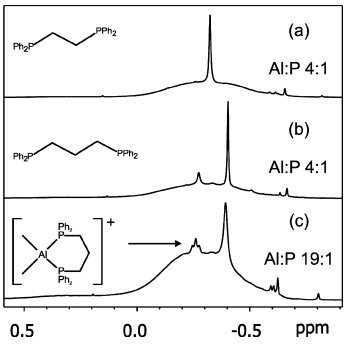

Figure 2. ^{1}H NMR spectra of MAO with dppe (a) and dppp (b, c). The Al/P ratio is reported as total Al present in the sample.

The addition of dppp to MAO in the ratio Al/P = 19/1 shows the expected shift of the TMA peak to higher field (δ −0.4), accompanied by a new triplet at δ −0.25 (J_{HP} = 4.4 Hz), which we attribute to the cationic complex $[Me_2Al(dppp)]^+$. Two peaks at δ −15.9 and −18.9 are seen in the ^{31}P NMR spectrum (free dppp: δ −15.7 in toluene). For comparison, the NMR spectra of a toluene solution of TMA and dppp (Al/P = 1/1) show a proton singlet at δ −0.26 and a ^{31}P signal at δ −15.8. The peak at δ −15.9 is therefore attributed to a TMA−dppp complex, while that at δ −18.9 can be related to the adduct between dppp and MAO. Adding increasing quantities of dppp to MAO solutions sharpens the ^{1}H TMA signal, while the triplet turns into a broad singlet and only one ^{31}P resonance is seen, at δ −19.9, diagnostic of a rapid exchange of dppp between the various available sites.

Indications for the presence of specific Lewis acidic sites in MAO capable of preferential binding of donor ligands are not only found with typical O, N, or P ligands. The addition of 1,2-difluorobenzene (FF) to MAO also leads to the formation of a well-defined triplet at δ −0.45 (J_{HF} = 2.4 Hz), although in this case the chemical shift does not change with increasing [FF] and there is no formation of a defined dissociated cationic dimethylaluminum complex in solution (see the Supporting Information).[40]

MAO Fractionation. The addition of L = $OPPh_3$, PMe_3, PCy_3 leads to the formation of TMA(L) adducts. At higher [L] these donors also induce the precipitation of the MAO polymer, leaving only the soluble TMA(L) complex in the supernatant. The oily MAO phase is soluble in solvents more polar than toluene, such as 1,2-difluorobenzene (FF) and THF (Figure 3). The ^{1}H NMR spectrum in FF of the precipitate obtained with $OPPh_3$ shows a broad signal between δ 0.2 and −0.8 due to the MAO component and a sharp peak at δ −0.72 attributable to

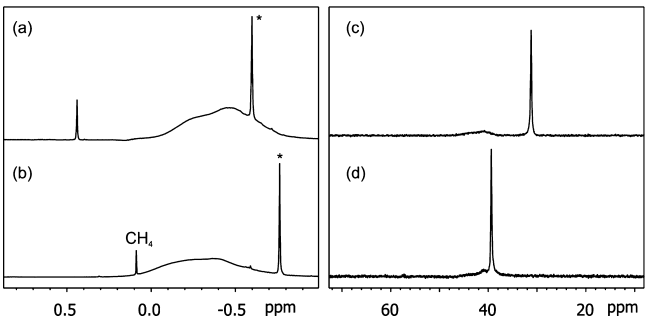

Figure 3. ^{1}H (a, b) and ^{31}P (c, d) NMR spectra in THF (a, c) and 1,2-difluorobenzene (FF; b, d) of the oily precipitate formed during the addition of $OPPh_3$ to MAO. The asterisk (*) denotes $AlMe_3$·$OPPh_3$.

dx.doi.org/10.1021/om4002878 | *Organometallics* XXXX, XXX, XXX−XXX

$AlMe_3{\cdot}OPPh_3$ (Figure 3b), as confirmed by the reaction of TMA with $OPPh_3$ (see the Experimental Section). The sharp peak at ca. δ 39.0 in the ^{31}P NMR spectrum is assigned to the compound $AlMe_3{\cdot}OPPh_3$ by comparison with Table 2, while the broad band at ca. δ 40 is most likely due to the $OPPh_3$ coordinated to MAO (Figure 3d). An analogous situation is observed in THF solution (Figure 3c).

Independent of the ligands used, the TMA content of the supernatant amounted to 2.6 ± 0.1 wt % and that of the precipitate 0.8 ± 0.05 wt % of the original MAO. Precipitation with these donor molecules therefore allows quantification of the "free" and "bound" TMA fractions: about three-fourths of the TMA is in toluene-soluble form, while the remaining one-fourth is associated with or entrapped in the MAO. On the other hand, precipitation of MAO with a stronger base, the phosphorus ylide $CH_2{=}PPh_3$, leads to the complete separation of TMA from the MAO polymer fraction (see the Supporting Information); this base is apparently able to break the MAO cages sufficiently to allow quantitative removal of any bound TMA.

Determination of the TMA Content by NMR Diffusion Coefficient and Small-Angle Neutron Scattering (SANS) Measurements. A series of pulsed field gradient spin echo (PFG-SE) NMR experiments of MAO solutions in toluene (Figure 4) allows the quantitative determination of diffusion coefficients and TMA and MAO concentrations.[41,42] Stejskal–Tanner plots of a concentration series of MAO (0.08% w/w ≤ $w(Al_{MAO})$ ≤10.7% w/w; Figure 4) clearly indicate the presence of a fast and a slow diffusing species for all concentrations. The peak integral between δ −0.8 and 0.6 of the ^1H NMR spectrum was used as the peak intensity. This area contains MAO signals as well as the overlapping TMA signal; therefore, they can be attributed to the slow and the fast diffusing species, respectively.

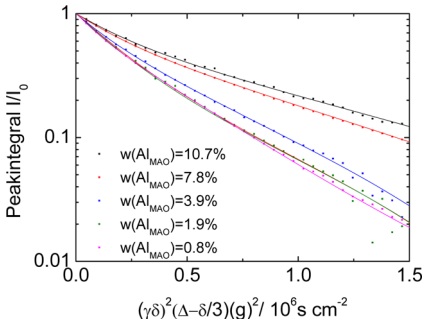

Figure 4. Stejskal–Tanner plot of a concentration series of MAO in toluene with a biexponential decay of the signal intensity, clearly indicating the presence of fast- and slow-diffusing species.

To analyze the data, a biexponential fit according to the Stejskal–Tanner plot of a concentration series is necessary (eq 2), where I/I_0 is the normalized peak intensity, $\chi(\mathrm{Me})$ is the mole fraction of methyl groups with $\chi(\mathrm{Me})_{TMA} = 1 - \chi(\mathrm{Me})_{MAO}$, D is the diffusion coefficient, γ is the gyromagnetic ratio, Δ is the diffusion length, δ is the gradient pulse length and g is the gradient.

$$\frac{I}{I_0}\chi(\mathrm{Me})_{TMA}\, e^{-D_{TMA}(\Delta-\delta/3)(\gamma\delta g)^2} + \chi(\mathrm{Me})_{MAO}\, e^{-D_{MAO}(\Delta-\delta/3)(\gamma\delta g)^2} \quad (2)$$

To take concentration effects into account, in a first approach each concentration was fitted separately according to eq 2, which reveals that for the two lowest concentrations under investigation the obtained parameters are constant within an experimental error of 4%. In particular, the constant $D_{toluene}$, which was used as the internal viscosity standard, ensures a dilute regime and consequently a solution viscosity equal to that of pure toluene.

To increase the number of experimental data points and therefore to improve fit stability and quality, we finally performed a simultaneous fit of all measured concentrations. Here $\chi(\mathrm{Me})$ is set as a global fit parameter (the same value for all concentrations), whereas $D(c)$ is allowed to vary with concentration. As Table 2 shows, the simultaneous fit reproduces the results of the THF addition quantitatively with respect to $\chi(\mathrm{Me})$. This validates the application of PFG experiments to quantify TMA concentrations within a complex MAO solution. It is striking that the D_{TMA} value in a dilute MAO solution is strongly reduced in comparison to that for a TMA solution in toluene ($D'_{TMA} = (10.4 \pm 0.38) \times 10^{-6}$ cm^2 s^{-1} and $D_{TMA} = (12.86 \pm 0.28) \times 10^{-6}$ cm^2 s^{-1} at $w(Al)$ = 1% w/w, respectively). For dilute solutions it is reasonable to assume that D_{TMA} is identical with the diffusion coefficient of TMA in toluene. With regard to the concept of free and associated TMA, this slowing down of TMA can be explained by a fast exchange of these two species. The measured value of D_{TMA} is a composition of a fraction of fast-diffusing TMA and a fraction of TMA with the same diffusion coefficient as MAO (eq 3). Consequently, a 75%

$$D'_{TMA} = \chi(\mathrm{TMA_{free}})D_{TMA} + (1 - \chi(\mathrm{TMA_{free}}))D_{MAO} \quad (3)$$

fraction of TMA diffuses quickly, whereas a 25% fraction of TMA is bound to MAO. Several experiments with different diffusion times Δ (50–200 ms) have been performed to estimate the exchange rate of this process.[43] Even at Δ = 50 ms there are no effects observable on the diffusion behavior of TMA. Therefore, the exchange process is too fast to be seen directly with PFG experiments.

Therefore, PFG-NMR experiments of MAO are a means not only of determining the total TMA content but also of distinguishing quantitatively between associated and free TMA. These results are in excellent agreement with those obtained independently from the phosphine addition studies; both techniques demonstrate that about 25% of TMA is "bound" or associated to MAO.[41]

The interpretation of diffusion coefficients D in terms of a hydrodynamic radius R_h via the Stokes–Einstein equation ($R_h \propto D^{-1}$) assuming a spherical structure raises several problems.[44] Different calibration methods (see the Supporting Information) give a hydrodynamic radius for MAO in toluene: $R_h(\mathrm{MAO}) \approx 12 \pm 0.3$ Å. If one assumes a dense spherical shape of MAO polymers, a comparison of volumes based on this experimental hydrodynamic radius with the volumes of calculated structures for methyl-rich MAO $[AlMe_{1.5}O_{0.75}]_n$ (i.e., a composition close to the experimentally determined Al/Me ratio of typical MAO) suggests that an MAO polymer molecule contains about 80–100 Al atoms (see the Supporting Information). This estimate is somewhat smaller than that by Babushkin and Brintzinger for zirconocene cations paired with [Me-MAO]$^-$ anions (150–200 Al atoms).[6h] However, such estimates depend strongly on the method used to calculate the volume: for example, volumes circumscribed by a limiting electron density (where the molecular volume is defined as a volume inside a contour of 0.001 e/bohr^3) or volumes taking steric hindrance and geometric constraints into account (e.g., the cube method, which takes into

dx.doi.org/10.1021/om4002878 | Organometallics XXXX, XXX, XXX–XXX

Table 2. Mole Fractions of Methyl Groups and the Diffusion Coefficients of MAO and TMA in a Dilute MAO Sample ($w(Al_{MAO})$ = 0.8% w/w)

method	$\chi(Me)_{TMA}$	D_{TMA}, 10^{-6} cm^2 s^{-1}	$\chi(Me)_{MAO}$	D_{MAO}, 10^{-6} cm^2 s^{-1}
THF addition	0.31		0.69	
PFG NMR simultaneous fit	0.31 ± 0.01	10.40 ± 0.38	0.71 ± 0.01	3.06 ± 0.04

account all solvent-inaccessible cavities within a given structure).[45,46] In fact, a detailed comparison for a well-characterized compound, the polyhedral oligomeric silsesquioxane isooctyl-POSS, reveals a factor of about 2 between measured (3053 Å^3 by PFG-NMR) and calculated volumes (2304 Å^3 by the cube method, 1662 Å^3 by electron density) (see the Supporting Information). Therefore, if the number of Al atoms per MAO polymer is deduced from dividing an experimental volume by the calculated volume per Al structural unit, this uncertainty has to be taken into account. The number of Al atoms per MAO should therefore be corrected by the empirically determined factor of 1.8, which results in an average of about 50−60 Al atoms per MAO polymer.

Determination of the MAO Molecular Weights and TMA Content by Small-Angle Neutron Scattering (SANS) Measurements. The hydrodynamic radius obtained by PFG-SE NMR methods could be confirmed independently by small-angle neutron scattering (SANS) experiments on a dilute MAO solution in toluene. Analysis of the SANS data give the radius of gyration of the MAO-TMA adduct as R_g = 9.3 ± 0.2 Å, which can be converted into the sphere radius $R_S = \sqrt{(5/3)}R_g$ = 12.0 ± 0.3 Å, in excellent agreement with PFG-NMR experiments. The good agreement between fitted model and experimental SANS data is shown in Figure 5; details of the analysis can be found in the Supporting Information.

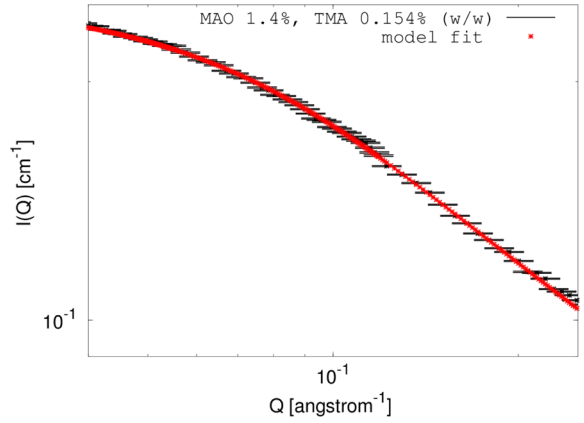

Figure 5. SANS intensity $I(Q)$ in absolute units (cm^{-1}) vs scattering vector Q for a dilute MAO solution in toluene.

Moreover, in combination with chemical analysis and NMR results, SANS results suggest an average molecular weight of MAO (without "bound" TMA) of 1800 ± 100. Taking the stoichiometric formula of MAO to be $Al(CH_3)_{1.5}O_{0.75}$, the number of Al atoms in a MAO polymer can be calculated to be 1800/60 ≈ 30. This number is about 50% less than the number estimated from our NMR results; however, considering the approximations involved in obtaining this estimate, the agreement is good.

In addition, we can calculate the average number of TMA molecules bound to one MAO polymer, N_{TMA}, from

$$\text{bound fraction} = N_{TMA}(m_{MAO}/M_{MAO})/(m_{TMA}/M_{TMA})$$

where M_{MAO} and M_{TMA} are molecular masses of MAO and TMA and m_{MAO} and m_{TMA} are their respective mass fractions in solution. The resulting value is $N_{TMA} \approx 0.78$; a similar number, $N_{TMA} \approx 0.64$, also results from analysis of the slow component in the PFG NMR data. One can speculate whether this number, i.e. approximately one TMA per MAO polymer, might indicate that there is only one special site per MAO polymer which interacts with TMA and which may be the site responsible for catalyst activation.

Computational Modeling of the MAO−THF Interaction. As the results discussed above have shown, MAO contains some structural elements that are capable of reacting with donor molecules with liberation of $[AlMe_2L_2]^+$ cations. We have explored the potential origin of these intriguing species by modeling the formation of THF−MAO adducts and the concomitant release of $[AlMe_2]^+$ cations.

The reaction of THF with MAO was explored by first focusing on small MAO polymers, likely produced during the initial steps of TMA hydrolysis. The MAOs are described by the structural formula $(AlMeO)_n(AlMe_3)_m$, and we chose species with (n,m) = (1,1), (1,2), (1,3), (2,2) as a starting point of the investigation. After classification of $AlMe_2$ centers in the MAOs according to their chemical environment by taking into account the neighboring oxygen atoms, we investigated the reaction of THF with the centers producing THF−MAO species. In the classification, C refers to terminal methyl and C^b to bridging methyl, while the number in parentheses after O gives its coordination number. The ring suffix refers to an Al species in a 4-membered Al_2O_2 ring. The MAO models and optimized molecular structures of the THF−MAOs are illustrated in Figure 6, whereas the calculated reaction energetics and the identified Al centers are given in Table 3.

The first interaction of Al_2Me_6 with THF leads to $Me_3Al(\mu$-$Me)AlMe_2(THF)$ (Figure 6, (0,2)). This is a local minimum; the further reaction to $^1/_2Al_2Me_6 + AlMe_3(THF)$ is exergonic, with ΔG = −54 kJ mol^{-1}. THF coordinates to the MAOs via the formation of an Al−O bond. The adduct formation is spontaneous for the MAOs except for the (1,3) species and $AlC_2O(3)_2$-ring site in (2,2). The unfavorable reaction with the $AlC_2C^bO(4)$ site of the (1,3) MAO originates from the already preferable 4-coordination of the Al atom in the MAO. Reaction of an analogous Al center in (1,2) is favorable due to structural distortion, which produces structurally analogous species for the THF−(1,2) adducts. The Al−O distance from the Al center to O in MAO (shown by r_{Al-O} in Table 3) provides a measure of the feasibility of the formation of $[Me_2Al(THF)_2]^+[MAO]^-$ cation−anion separation. The largest separation is obtained for (1,3), because the oxygen atom neighboring the Al center is 4-coordinated and the elongation of this Al−O bond to form a 3-coordinate O is energetically favorable.[16]

Anionization potentials, i.e. energies of the reactions MAO → $[AlMe_2]^+ + [MAO]^-$, provide a computationally practical way to probe the feasibility of anion formation. A detailed analysis of MAOs produced by hydrolysis of TMA is in progress, which will

dx.doi.org/10.1021/om4002878 | Organometallics XXXX, XXX, XXX−XXX

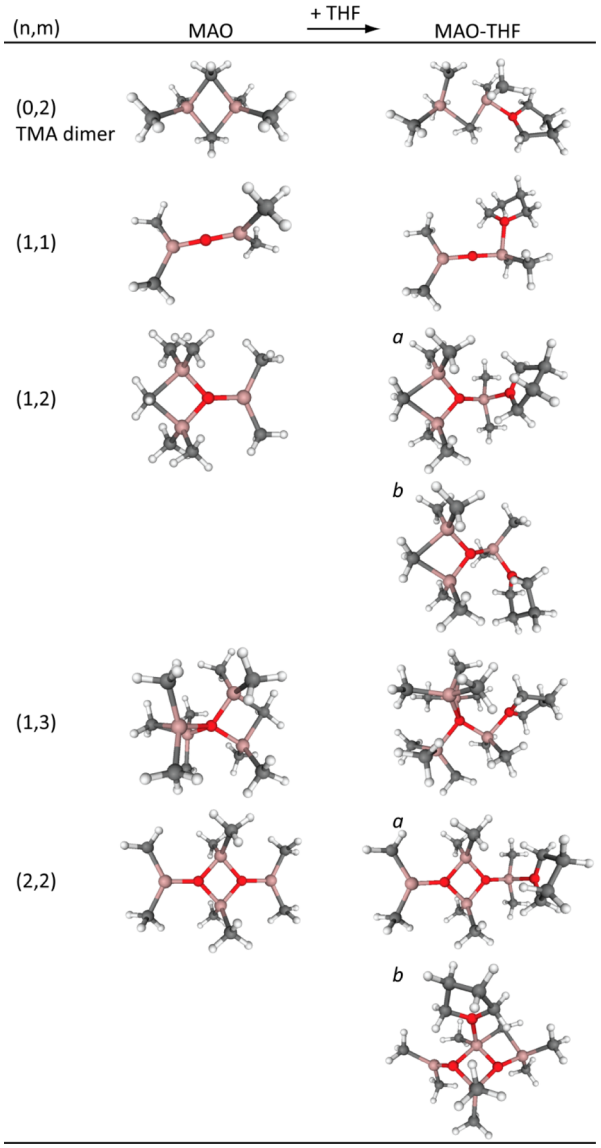

Figure 6. Models for $(AlMeO)_n(AlMe_3)_m$ MAOs labeled according to (n,m) and structures of the MAO + THF → MAO−THF reaction products. Structural isomers are distinguished by *a* and *b*. H, C, O, and Al atoms are illustrated in white, gray, red, and pink, respectively.

Table 3. RI-MP2/TZVP-Calculated Standard Gibbs Energies of the Reaction MAO + THF → MAO−THF (T = 298 K), $(AlMeO)_n(AlMe_3)_m$ MAOs, Chemical Environments of the Al Centers, and Al Center−O(MAO) Distances (r_{Al-O})

(n,m)	Al center	ΔG (kJ/mol)	r_{Al-O} (Å)[a]
(0,2) TMA dimer	$AlC_2C_2^b$	−3.3	
(1,1)	$AlC_2O(2)$	−74.0	1.737
(1,2)-*a*	$AlC_2O(3)$	−92.7	1.793
(1,2)-*b*	$AlC_2C^bO(4)$	−87.7	1.796
(1,3)	$AlC_2C^bO(4)$	1.0	1.903
(2,2)-*a*	$AlC_2O(3)$	−88.0	1.791
(2,2)-*b*	$AlC_2O(3)_2$-ring	5.6	1.856

[a]Where Al is bound to two oxygen atoms, an average of the two Al−O bond distances is reported.

provide potential MAO sources for $[AlMe_2]^+$ abstraction.[47] Figure 7 summarizes key preliminary findings regarding the anionization potentials of $(AlOMe)_n(AlMe_3)_m$, where $n \leq 8$.

The rearrangement of the anions following $[AlMe_2]^+$ dissociation is an important contributing factor to their stability. Both −O−$AlMe_2$−O− and −O−$AlMe_2$−μ-Me− structures are capable of generating $[AlMe_2]^+$, with no total energy difference due to structural rearrangement. Of these, the structure with (n,m) = (8,2) gives a particularly stable anion; this MAO model has an ideal environment for $[AlMe_2]^+$ abstraction from the $AlC_2C^bO(4)$ site. Also, cleavage of $[AlMe_2]^+$ removes the only methyl bridge, leaving a cage consisting solely of 4-coordinate Al, 3-coordinate O, and terminal methyl groups. The resulting structure has three Al_2O_2 4-membered rings, all separated by 6-rings, whereas energetically less favored structures contain edge- or corner-sharing 4-rings.

CONCLUSIONS

One of the most important characteristics of methylalumoxane that determines its reactivity as a catalyst activator, as well as its shelf life prior to catalyst preparation, is its trimethylaluminum content. MAO is a complex substance, and a combined chemical, spectroscopic, and computational approach has been employed to try and identify some key characteristics. A comparison confirmed that the addition of donor molecules such as THF, pyridine, and triphenylphosphine provides a consistent method of TMA quantification, while the addition of trialkylphosphines led to the precipitation of polymeric MAO and the partitioning of TMA into "free" and "bound" fractions. These results could be confirmed independently by pulsed field gradient NMR methods. Measurements of the diffusion coefficients of TMA and MAO can be used to determine the average hydrodynamic radius of MAO, data which are in close agreement with those obtained from small-angle neutron scattering. Conversion of these radii into molecular volumes for molecules of ill-defined geometry such as MAO is less straightforward; our estimates suggest that an MAO molecule contains about 30−60 Al atoms. It could be shown that MAO contains small amounts of structures which, on reaction with suitable bases, can lead to the dissociation of $[AlMe_2L_2]^+$ cations. Computational modeling has shown that these structures are likely to be associated with $Al_2(\mu$-$Me)(\mu$-$O)$ and $Al_2(\mu$-$O)_2$ 4-rings. Similar processes are highly likely involved in catalyst activation. The computations do indeed indicate that for larger MAO cages this ionization is becoming increasingly energetically feasible. The ability of the resulting anion to relax into a more stable cage structure contributes crucially to the overall energetics of this process, and cages where the 4-membered rings are isolated from one another by 6-rings are particularly favored. These studies lay the foundation for more detailed consideration of these processes on larger MAO models.

EXPERIMENTAL SECTION

Materials and Techniques. All manipulations were conducted under an inert atmosphere of dry argon using standard Schlenk techniques. All reagents were used as purchased without further purification unless otherwise stated. A solution of MAO (30 wt % MAO + TMA in toluene) was provided by Chemtura Organometallics GmbH. It was stored at −20 °C, and it was 10 months old at the time of analysis.

Solvents were dried over Na/benzophenone (tetrahydrofuran) or sodium (toluene) before use and purged with argon. 1,2-Difluorobenzene (FF, Apollo Scientific), extra-dry pyridine (Py, Acros), and PMe_3 (1 M in toluene, Sigma Aldrich) were degassed with a stream of argon and stored over activated 4 Å molecular sieves. Deuterated NMR solvents (CD_2Cl_2 and toluene-d_8) were degassed by several freeze−thaw cycles and dried over activated 4 Å molecular sieves. NMR spectra were recorded using a Bruker Avance DPX-300 spectrometer. ^{1}H (300 MHz)

dx.doi.org/10.1021/om4002878 | *Organometallics* XXXX, XXX, XXX−XXX

n	m	MAO	MAO^-	ΔE/ kJmol^{-1}	Al center
0	2	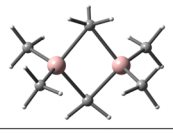	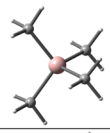	0.0	$AlC_2C_2^b$
1	3	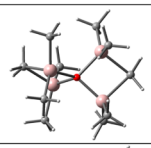	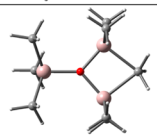	−49.5	$AlC_2C^bO(4)$
2	4	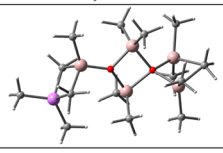	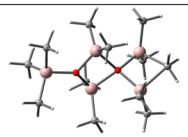	−93.2	$AlC_2C_2^b$
3	2	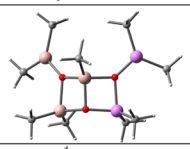	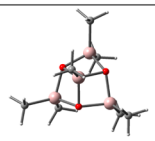	−60.9	$AlC_2O(3)$ and $AlC_2O(3)_2$
4	3	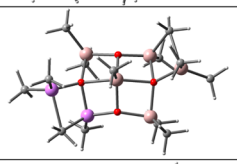	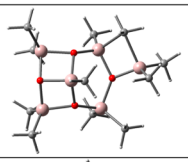	−63.5	$AlC_2C^bO(4)$ and $AlCC^bO(4)O(3)$
6	4	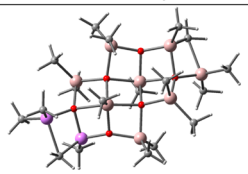	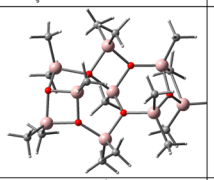	−117.9	$AlC_2C^bO(4)$ and $AlCC^bO(4)O(3)$
8	2	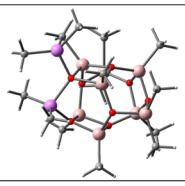	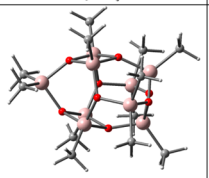	−162.8	$AlC_2C^bO(4)$ and $AlCC^bO(4)O(3)$

Figure 7. Anionization potentials of selected MAOs, $(AlOMe)_n(AlMe_3)_m$, relative to the TMA dimer: C^b, bridging methyl; $O(n)$, n-coordinate O; purple Al, site of $AlMe_2^+$ dissociation.

and ^{31}P NMR (121.5 MHz) chemical shifts were referenced to the residual solvent peaks of two separate external standards of CD_2Cl_2 and of H_3PO_4 (85% in H_2O), each contained in a capillary. 1,3,5-Tri-*tert*-butylbenzene was used as an internal standard. In order to compensate for sloping baselines and peak overlaps, the ^1H NMR signals were integrated by printing the spectra on A4 sheets of paper (80 g/m^2), cutting the peaks, and weighing on an analytical balance. Pulse delays (D_1) of 25 and 16 scans were used for ^1H NMR spectra. The D_1 value was chosen in line with the longer proton NMR relaxation times reported by Imhoff et al. for MAO solutions.[3]

Diffusion experiments were performed on a Varian Inova 400 spectrometer. All measurements were carried out at 293 ± 1 K; during an experiment the temperature was stable within 0.1 K. The Dbppste_CC (DOSY bipolar pulse pair stimulated echo with convection compensation) pulse program was used.[4] The diffusion time Δ was adjusted (typically 20 and 200 ms); the gradient pulse length δ was 2 ms. The number of transients was adjusted to the concentration.

Small-angle neutron scattering (SANS) experiments were performed with a KWS-2 instrument (JCNS Outstation, FRM II, Munich, Germany). We measured an MAO solution in a toluene/d_8-toluene mixture with the following concentrations (w/w): MAO, 1.39%; TMA, 0.17%; toluene, 3.8%; toluene-d_8 94.57%.

Computational Details. The MAO−THF calculations were performed by the RI-MP2 method[48−51] in combination with the def-TZVP basis set,[52] as implemented in TURBOMOLE version 6.3.[53] The structures were fully optimized and verified as true local minima by determining their vibrational frequencies, also required for calculation of Gibbs energies. No scaling factors were employed. NMR calculations were performed at the MP2/TZVP level of theory using the gauge-independent atomic orbital (GIAO) method as implemented in Gaussian09.[54] Fast rotation of the methyl groups was assumed in the NMR peak visualization. Anionization potentials, i.e. relative energies for the reaction MAO → $[AlMe_2]^+ + [MAO]^-$, were calculated by the density functional M062X/TZVP method.[55] Molecular volumes were defined as a volume inside a contour of 0.001 e/bohr^3 density and were calculated at the HF/SVP level[56] of theory for MAO models up to 148 Al atoms. The volumes and Cartesian coordinates of the MAOs are given in the Supporting Information.

Reactions and Syntheses. *Determination of the TMA Content in 30% MAO by THF and Py.* MAO (2 mL, 9.72 mmol Al) and THF (1.6−250 mmol) were stirred for 30 min at room temperature. An aliquot (0.5 mL) of the resulting solution was transferred to an NMR tube containing a CD_2Cl_2 capillary and 1,3,5-tri-*tert*-butylbenzene (10 − 40 μL, 0.5 *M* in toluene), and ^1H NMR spectra were recorded.

dx.doi.org/10.1021/om4002878 | *Organometallics* XXXX, XXX, XXX−XXX

Determination of TMA in MAO by PPh_3. MAO (2 mL, 9.72 mmol Al) and PPh_3 (1.18 g in 5 mL of toluene, 4.5 mmol) were stirred at room temperature for 1 h. An aliquot (50 μL) was transferred to an NMR tube containing toluene (0.5 mL) and capillaries with CD_2Cl_2 and H_3PO_4 (85%) to record ^1H and ^{31}P NMR spectra. The calibration curve (Figure S2, Supporting Information) was obtained by plotting the ^{31}P NMR chemical shifts of standard TMA/PPh_3 mixtures with Al/P molar ratios between 1/10 and 1/1. The following linear relationship was found:

$$Al/P = -0.2957\delta - 1.5378 \quad R = 0.997$$

where *Al* indicates the moles of $AlMe_3(PPh_3)$ and *P* the moles of PPh_3 added to the solution.

Reaction of MAO with $OPPh_3$, PCy_3, and PMe_3. $OPPh_3$, PCy_3, or PMe_3 (0.5−5 mL, 1 M in toluene) and MAO (30% in toluene; 2 mL, 9.72 mmol of Al) were stirred at room temperature for 30 min. A clear colorless oil precipitated, and the suspension was decanted. An aliquot (0.5 mL) of the supernatant solution was studied by ^1H and ^{31}P NMR using CD_2Cl_2 and H_3PO_4 (85%) capillaries and 1,3,5-tri-*tert*-butylbenzene as internal standard (10−40 μL, 0.5 M in toluene). The oil was washed with toluene (2 × 5 mL) and dissolved in THF or 1,2-difluorobenzene (2 mL). An aliquot of the solution was transferred to an NMR tube, again containing CD_2Cl_2 and H_3PO_4 (85%) capillaries and 1,3,5-tri-*tert*-butylbenzene (20 μL, 0.5 M in toluene). The ^1H and ^{31}P NMR spectra were recorded.

^1H NMR of TMA(L): L = PMe_3, δ −0.41, C_6D_6;[8] L = PCy_3, δ −0.19, C_6D_6;[9] L = $OPPh_3$, δ− 0.3, toluene. In the case of PMe_3, a broad ^{31}P NMR signal at δ −8.0 is observed which is not a weighted average of PMe_3 and $AlMe_3(PMe_3)$. This signal may be due to equilibria involving $OPMe_3$ (δ 36.2, C_6D_6), from the partial oxidation of PMe_3. Adding $OPPh_3$ ($\delta(^{31}P)$ 24.3) to MAO results in a slightly broad ^{31}P signal at δ 27.0, due to a fast exchange between $OPPh_3$ and $AlMe_3(OPPh_3)$.

■ ASSOCIATED CONTENT

Ⓢ Supporting Information

Text, figures, and tables giving experimental and spectroscopic details, details for SANS and PFG NMR measurements, optimized structures for calculated molecular volumes, and coordinates for calculated structures. This material is available free of charge via the Internet at http://pubs.acs.org.

■ AUTHOR INFORMATION

Corresponding Author

*M.B.: tel, +44 1603 592044; e-mail, m.bochmann@uea.ac.uk. M.L.: e-mail, mikko.linnolahti@uef.fi. J.S.: e-mail, j.stellbrink@fz-juelich.de.

Notes

The authors declare no competing financial interest.

■ ACKNOWLEDGMENTS

This work was supported by the European Commission (Grant NMP4-SL-2010-246274). We thank Chemtura Organometallics GmbH for samples of methylaluminoxane. The computations were made possible by use of the Finnish Grid infrastructure resources.

■ REFERENCES

(1) (a) Sinn, H. *Macromol. Symp.* **1995**, *97*, 27. (b) Kaminsky, W. *Macromol. Symp.* **1995**, *97*, 79. (c) Sinn, H.; Kaminsky, W.; Vollmer, H. J.; Woldt, R. *Angew. Chem., Int. Ed. Engl.* **1980**, *19*, 390. (d) Sinn, H.; Kaminsky, W. *Adv. Organomet. Chem.* **1980**, *18*, 99.

(2) Severn, J. R. In *Tailor-Made Polymers. Via Immobilization of Alpha-Olefin Polymerization Catalysts*; Wiley-VCH: Weinheim, Germany, 2008, p 95.

(3) Babushkin, D. E.; Semikolenova, N. V.; Panchenko, V. N.; Sobolev, A. P.; Zakharov, V. A.; Talsi, E. P. *Macromol. Chem. Phys.* **1997**, *198*, 3845.

(4) (a) Tritto, I.; Sacchi, M. C.; Locatelli, P.; Li, S. X. *Macromol. Chem. Phys.* **1996**, *197*, 1537. (b) Tritto, I.; Mealares, C.; Sacchi, M. C.; Locatelli, P. *Macromol. Chem. Phys.* **1997**, *198*, 3963.

(5) Smith, G. M.; Malpass, D. B.; Bernstein, S. N.; Jones, P. D.; Monfiston, D. J.; Rogers, J.; Su, B. M.; Palmaka, S. W.; Tirendi, C. F.; Crapo, C. C.; Deavenport, D. L.; Hodges, J. T.; Ngo, R. H.; Post, C. W.; Rabbitt, C. S. *Proc. Polyolefins X - 10th Internat. Conf. Polyolefins* **1997**, 49.

(6) For equilibria in MAO-activated metallocene catalysts see for example: (a) Tritto, I.; Li, S. X.; Sacchi, M. C.; Locatelli, P.; Zannoni, G. *Macromolecules* **1995**, *28*, 5358. (b) Tritto, I.; Donetti, R.; Sacchi, M. C.; Locatelli, P.; Zannoni, G. *Macromolecules* **1997**, *30*, 1247. (c) Babushkin, D. E.; Semikolenova, N. V.; Zakharov, V. A.; Talsi, E. P. *Macromol. Chem. Phys.* **2000**, *201*, 558. (d) Bryliakov, K. P.; Semikolenova, N. V.; Yudaev, D. V.; Ystenes, M.; Rytter, E.; Zakharov, V. A.; Talsi, E. P. *Macromol. Chem. Phys.* **2003**, *204*, 1110. (e) Bryliakov, K. P.; Semikolenova, N. V.; Yudaev, D. V.; Zakharov, V. A.; Brintzinger, H. H.; Ystenes, M.; Rytter, E.; Talsi, E. P. *J. Organomet. Chem.* **2003**, *683*, 92. (f) Wieser, U.; Schaper, F.; Brintzinger, H. H. *Macromol. Symp.* **2006**, *236*, 63. (g) Babushkin, D. E.; Naundorf, C.; Brintzinger, H. H. *Dalton Trans.* **2006**, 4539. (h) Babushkin, D. E.; Brintzinger, H. H. *J. Am. Chem. Soc.* **2002**, *124*, 12869. (i) Bryliakov, K. P.; Semikolenova, N. V.; Panchenko, V. N.; Zakharov, V. A.; Brintzinger, H. H.; Talsi, E. P. *Macromol. Chem. Phys.* **2006**, *207*, 327. (j) Babushkin, D. E.; Brintzinger, H. H. *Chem. Eur. J.* **2007**, *13*, 5294. (k) Bryliakov, K. P.; Talsi, E. P.; Voskoboynikov, A. Z.; Lancaster, S. J.; Bochmann, M. *Organometallics* **2008**, *27*, 6333.

(7) (a) Kleinschmidt, R.; van der Leek, Y.; Reffke, M.; Fink, G. *J. Mol. Catal. A: Chem.* **1999**, *148*, 29. (b) Jüngling, S.; Mülhaupt, R. *J. Organomet. Chem.* **1995**, *497*, 27. (c) Reddy, S. S.; Radhakrishnan, K.; Sivaram, S. *Polym. Bull. (Berlin)* **1996**, *36*, 165.

(8) Matsui, S.; Mitani, M.; Saito, J.; Tohi, Y.; Makio, H.; Matsukawa, N.; Takagi, Y.; Tsuru, K.; Nitabaru, M.; Nakano, T.; Tanaka, H.; Kashiwa, N.; Fujita, T. *J. Am. Chem. Soc.* **2001**, *123*, 6847.

(9) See for example: Quevedo-Sanchez, B.; Nimmons, J. F.; Coughlin, E. B.; Henson, M. A. *Macromolecules* **2006**, *39*, 4306.

(10) Pasynkiewicz, S. *Polyhedron* **1990**, *9*, 429.

(11) (a) Panchenko, V. N.; Zakharov, V. A.; Danilova, I. G.; Paukshtis, E. A.; Zakharov, I. I.; Goncharov, V. G.; Suknev, A. P. *J. Mol. Catal. A: Chem.* **2001**, *174*, 107. (b) Zakharov, V. A.; Zakharov, I. I.; Panchenko, V. N. In *Organometallic Catalysts and Olefin Polymerization*; Springer: Berlin, 2001; pp 63−71.

(12) (a) Talsi, E. P.; Semikolenova, N. V.; Panchenko, V. N.; Sobolev, A. P.; Babushkin, D. E.; Shubin, A. A.; Zakharov, V. A. *J. Mol. Catal. A: Chem.* **1999**, *139*, 131. (b) Pedeutour, J. N.; Radhakrishnan, K.; Cramail, H.; Deffieux, A. *Macromol. Rapid Commun.* **2001**, *22*, 1095.

(13) (a) Zurek, E.; Ziegler, T. *Prog. Polym. Sci.* **2004**, *29*, 107. (b) Zurek, E.; Ziegler, T. *Inorg. Chem.* **2001**, *40*, 3279.

(14) (a) Glaser, R.; Sun, X. *J. Am. Chem. Soc.* **2011**, *133*, 13323. (b) van Rensburg, W. J.; van den Berg, J. A.; Steynberg, P. J. *Organometallics* **2007**, *26*, 1000.

(15) (a) Ystenes, M.; Eilertsen, J. L.; Liu, J. K.; Ott, M.; Rytter, E.; Stovneng, J. A. *J. Polym. Sci., Part A: Polym. Chem.* **2000**, *38*, 3106. (b) Zakharov, I. I.; Zakharov, V. A.; Potapov, A. G.; Zhidomirov, G. M. *Macromol. Theory Simul.* **1999**, *8*, 272.

(16) Linnolahti, M.; Severn, J. R.; Pakkanen, T. A. *Angew. Chem., Int. Ed.* **2008**, *47*, 9279.

(17) Hansen, E. W.; Blom, R.; Kvernberg, P. O. *Macromol. Chem. Phys.* **2001**, *202*, 2880.

(18) Imhoff, D. W.; Simeral, L. S.; Sangokoya, S. A.; Peel, J. H. *Organometallics* **1998**, *17*, 1941.

(19) For an early example of this structural type see: Atwood, J. L.; Hrncir, D. C.; Priester, R. D.; Rogers, R. D. *Organometallics* **1983**, *2*, 985.

(20) (a) Harlan, C. J.; Bott, S. G.; Barron, A. R. *J. Am. Chem. Soc.* **1995**, *117*, 6465. (b) Mason, M. R.; Smith, J. M.; Bott, S. G.; Barron, A. R. *J. Am. Chem. Soc.* **1993**, *115*, 4971. (c) Harlan, C. J.; Mason, M. R.; Barron, A. R. *Organometallics* **1994**, *13*, 2957.

(21) Watanabi, M.; McMahon, C. N.; Harlan, C. J.; Barron, A. R. *Organometallics* **2001**, *20*, 460.

(22) Ghiotto, F.; Pateraki, C.; Severn, J. R.; Friederichs, N.; Bochmann, M. *Dalton Trans.* **2013**, DOI: 10.1039/C3DT00107E.

(23) (a) Bochmann, M.; Lancaster, S. J. *Angew. Chem., Int. Ed. Engl.* **1994**, *33*, 1634. (b) Bochmann, M.; Lancaster, S. J. *J. Organomet. Chem.* **1995**, *497*, 55.
(24) (a) Wu, Q.; Ye, Z.; Gao, Q. H.; Lin, S. G. *Macromol. Chem. Phys.* **1998**, *199*, 1715. (b) Reddy, S. S.; Sivaram, S. *Prog. Polym. Sci.* **1995**, *20*, 309. (c) Reddy, S. S.; Shashidhar, G.; Sivaram, S. *Macromolecules* **1993**, *26*, 1180. (d) Chien, J. C. W.; Wang, B.-P. *J. Polym. Sci., Part A: Polym. Chem.* **1988**, *26*, 3089.
(25) Tynys, A.; Eilertsen, J. L.; Seppala, J. V.; Rytter, E. *J. Polym. Sci., Part A: Polym. Chem.* **2007**, *45*, 1364.
(26) Busico, V.; Cipullo, R.; Cutillo, F.; Friederichs, N.; Ronca, S.; Wang, B. *J. Am. Chem. Soc.* **2003**, *125*, 12402.
(27) Turunen, J. P. J.; Pakkanen, T. T. *J. Appl. Polym. Sci.* **2006**, *100*, 4632.
(28) Jordon, D. E. *Anal. Chem.* **1968**, *40*, 2150.
(29) Resconi, L.; Bossi, S.; Abis, L. *Macromolecules* **1990**, *23*, 4489.
(30) Barron, A. R. *Organometallics* **1995**, *14*, 3581.
(31) Eilertsen, J. L.; Rytter, E.; Ystenes, M. *Vib. Spectrosc.* **2000**, *24*, 257.
(32) Bliemeister, J.; Hagendorf, W.; Harder, A.; Heitmann, B.; Schimmel, I.; Schmedt, E.; Schnuchel, W.; Sinn, H.; Tikwe, L.; Vonthienen, N.; Urlass, K.; Winter, H.; Zarncke, O. In *Ziegler Catalysts: Recent Scientific Innovations and Technological Improvements*; Springer: Heidelberg, Germany, 1995; pp 57−82.
(33) Luo, L.; Sangokoya, S. A.; Wu, X.; Diefenbach, S. P.; Kneale, B. U.S. Pat. Appl. 2009/0062492 A1 (2009, Albemarle Corp.).
(34) Another recent patent refers to an "unknown species present in MAO" observed after THF addition, i.e. $[AlMe_2(THF)_2]^+$, and correlates the concentration of this species and of TMA with the composition and molecular weights of the ethylene copolymers: Crowther, D. J.; Fiscus, D. M. PCT Int. Appl. WO2012/096698 (2012, Exxon Mobil).
(35) (a) Klosin, J.; Roof, G. R.; Chen, E. Y.-X. *Organometallics* **2000**, *19*, 4684. (b) Klosin, J. PCT Int. Appl. WO2000/11006 (2000, Dow Chemical Co.). (c) Chen, E. Y.-X.; Kruper, W. J.; PCT Int. Appl. WO 2001/5642 (2001, Dow Chemical Co.).
(36) Bochmann, M.; Sarsfield, M. J. *Organometallics* **1998**, *17*, 5908.
(37) Yamashita, Y.; Kasahara, H.; Suyama, K.; Okada, M. *Makromol. Chem.* **1968**, *117*, 242.
(38) For Al/THF = 6/1, the value of TMA is slightly lower, probably due to the fact that there is not enough THF to extract all the TMA ("free" and "bound") or due to the partial overlapping of the $AlMe_3$·THF signal with an unidentified species (see the shoulder of the * signal in Figure 1; Al/THF = 6/1), which affects the integration value.
(39) Similar solvent-induced ^{1}H NMR shifts of the Al-Me signal are observed for $[AlMe_2(THF)_2][MeB(C_6F_5)_3]$: δ −0.94 ppm in toluene, −0.25 ppm in THF, and −0.45 ppm in toluene/THF (1/2 v/v).
(40) Attempts to generate $[AlMe_2(1,2\text{-difluorobenzene})]^+$ cations from $AlMe_3$ and $B(C_6F_5)_3$ in difluorobenzene/toluene produced no reaction at room temperature and only decomposition products at 40 °C.
(41) The measured diffusion coefficient of MAO, D_{MAO} = (3.06 ± 0.04) 10^{-6} cm^2 s^{-1}, at high dilution is in excellent agreement with the results of Hansen et al. (D_{MAO} = (3.1 ± 0.1) 10^{-6} cm^2 s^{-1}); however, these authors decreased the TMA content to $\chi(Me_{TMA}) = 0.09 \pm 0.01$ and completely neglected the influence of the residual TMA.[17]
(42) Rocchigiani, L.; Busico, V.; Pastore, A.; Macchioni, A. *Dalton Trans.* **2013**, DOI: 10.1039/C3DT00041A.
(43) Kärger, J.; Pfeifer, H.; Heink, W. In *Advances in Magnetic Resonance*; Waugh, J., Ed.; Academic Press: New York, 1988; Vol. *12*, pp 1−89.
(44) Macchioni, A.; Ciancaleoni, G.; Zuccaccia, C.; Zuccaccia, D. *Chem. Soc. Rev.* **2008**, *37*, 479.
(45) Müller, J. J. *J. Appl. Crystallogr.* **1983**, *16*, 74.
(46) Kusmin, A.; Lechner, R. E.; Kammel, M.; Saenger, W. *J. Phys. Chem. B* **2008**, *112*, 12888.
(47) Linnolahti, M.; Laine, A.; Pakkanen, T. A. *Chem. Eur. J.* **2013**, *19*, 7133.
(48) Hattig, C. J. *Chem. Phys.* **2003**, *118*, 7751.
(49) Weigend, F.; Haser, M.; Patzelt, H.; Ahlrichs, R. *Chem. Phys. Lett.* **1998**, *294*, 143.
(50) Hattig, C.; Hellweg, A.; Kohn, A. *Phys. Chem. Chem. Phys.* **2006**, *8*, 1159.
(51) Hattig, C.; Weigend, F. *J. Chem. Phys.* **2000**, *113*, 5154.
(52) Schäfer, A.; Huber, C.; Ahlrichs, R. *J. Chem. Phys.* **1994**, *100*, 5829.
(53) *TURBOMOLE V6.3 2011*, a Development of University of Karlsruhe and Forschungszentrum Karlsruhe GmbH, 1989−2007, TURBOMOLE GmbH, since 2007; available from http://www.Turbomole.Com.
(54) Frisch, M. J., et al. *Gaussian 09, Revision A.02*; Gaussian, Inc., Wallingford, CT, 2009.
(55) Zhao, Y.; Truhlar, D. G. *Theor. Chem. Acc.* **2008**, *120*, 215.
(56) Schäfer, A.; Horn, H.; Ahlrichs, R. *J. Chem. Phys.* **1992**, *97*, 2571.